Environmental Science Water Research & Technology



PAPER

View Article Online



Cite this: Environ. Sci.: Water Res. Technol., 2023, 9, 2836

Emerging investigator series: post-synthesis modification of reverse osmosis membranes for the enhanced separation of small neutral molecules†

Shahriar Habib, Madison A. Wilkins and Steven T. Weinman **D**



Reverse osmosis (RO) membranes are used ubiquitously for seawater desalination. Ideally, the interfacial polymerization (IP) reaction used to synthesize RO membranes would form a uniform pore or free volume element structure within the polyamide layer. In reality, the self-limiting and chaotic nature of IP prevents the saturation of the RO active layer with the aqueous reactant. Unexploited attachment sites on the organic reactant are negatively charged in an aqueous solution, facilitating the desalination apt of RO membranes. However, these unreacted sites leave the pore structure with sizeable free-volume holes which permit small, neutral molecules (SNMs) to permeate through the membrane. The goal of this research is to decrease free volume space on the surface of the polyamide layer to improve the size exclusion properties of RO membranes and SNM rejection. We hypothesize that conjugating diamines or a branched polyamine to the synthesized polyamide layer will increase cross-linking to facilitate this improvement. To test this hypothesis, the polyamide layer of a commercial RO membrane is activated using carbodiimide chemistry and subsequently modified with an amine. Then, the modified membranes are heat treated in a microwave or hot water bath. The effects of various amines including 1,6-diaminohexane, 1,8-diaminooctane, m-phenylenediamine, and polyethyleneimine (10 000 MW) are evaluated. The results show that combining the application of amine conjugation and heat treatment significantly improves SNM rejection. Specifically, urea rejection was increased from 21% to 61%, and boron rejection was increased from 23% to 59%

Received 31st May 2023, Accepted 5th October 2023

DOI: 10.1039/d3ew00401e

rsc.li/es-water

Water impact

Current reverse osmosis membranes are poor at removing small neutral molecules from water. This work has resulted in a notable improvement in a commercial reverse osmosis membrane rejection of small neutral molecules by using carbodiimide chemistry to activate the membrane surface for amine coupling and heat treatment. The membrane urea and boric acid removal was improved from 20% to 60%.

1. Introduction

Beginning in the late 1950's, reverse osmosis (RO) membranes have been studied as tools to combat the scarcity of potable, clean water. 1,2 Since then, RO membranes have been used ubiquitously for seawater desalination.3 The desalination performance of RO membranes stems from the interfacial polymerization (IP) reaction used to synthesize them. During this process, the polyamide layer is formed at the interface of two immiscible phases: aqueous m-phenylene diamine (MPD)

Department of Chemical and Biological Engineering, The University of Alabama, Tuscaloosa, AL 35487, USA. E-mail: stweinman@eng.ua.edu; Fax: +1 (205) 348 7558; Tel: +1 (205) 348 8516

and organic trimesoyl chloride (TMC). Due to its slight solubility in the organic phase, MPD diffuses from the aqueous to the organic phase.4,5 This diffusion allows MPD to react with TMC at the interface to generate the polyamide layer of RO membranes.⁶ Ideally, IP would generate a uniform pore free volume element structure (known as network pores) within the polyamide layer. However, in reality, this reaction is rapid, uncontrolled, and semi self-limiting.^{7,8} Due to the uncontrollable nature of this reaction, the pore structure contains not fully reacted TMC (and likely some MPD) molecules leading to larger free volume space (known as aggregate pores).9

Conveniently, incomplete IP contributes to the excellent charge-exclusion properties of RO membranes. When TMC molecules encounter the aqueous phase, acid chloride groups which do not form amide bonds with MPD hydrolyze to generate carboxylic acid groups. These acid groups are

[†] Electronic supplementary information (ESI) available. See DOI: https://doi.org/ 10.1039/d3ew00401e

[‡] These authors contributed equally to this work.

negatively charged in an aqueous solution at a pH > 4.0. Due to charge repulsion, these increased negative charges on the surface of the RO membrane make the membrane able to repel anions, such as chloride. 11 By more effectively rejecting anions, the membrane also effectively rejects salt counter ions, like sodium, per the principles of membrane equilibria. 12 Therefore, the not fully reacted TMC molecules contribute to the impressive desalination ability of RO membranes.

While the self-limiting and chaotic nature of IP may contribute to charge-exclusion, it hinders the size-exclusion properties of RO membranes. TMC molecules that are not fully reacted break the expected chain of uniform network pores within the polyamide layer, resulting in larger aggregate free volume holes.9 Small, neutral molecules (SNMs) which do not respond to Donnan exclusion mechanisms can slip through this free volume space. 13 In this way, not fully reacted TMC molecules resulting from the incomplete IP between MPD and TMC squander the potential of RO membranes for use as a tool for SNM rejection.¹⁴

It is desired to improve the ability of RO membranes to effectively reject SNMs. SNMs of particular interest are urea and boric acid. Urea is used worldwide as a cheap source of nitrogen fertilizer, and its use has increased more than 100-fold in the last four decades. 15 Additionally, urea is used extensively in animal feeds and manufacturing processes. 15 The industrial shift towards using urea as an abundant and cheap source of nitrogen for these purposes parallels the increasing demand for food to feed the growing global population.¹⁵

Urea used for agriculture and livestock care is retained in soil, and overland transport allows urea to travel to both coastal and estuarine waters, elevating the total dissolved organic nitrogen amount to an environmentally unsafe level. 15 Elevated levels of dissolved organic nitrogen in coastal waters fuel harmful algal bloom species. Over time, harmful algal blooms can irreversibly damage marine ecosystems. Harmful algal blooms not only affect marine life, but they can also result in seafood which is toxic to human health.16 As a result of the increase in urea usage in the recent years, these adverse environmental effects of urea contaminated wastewater have become of particular concern.

Another relevant application of urea-rejecting RO membranes is the miniature, peritoneal dialysis artificial kidney. In these miniature dialysis devices, RO membranes may be used to eliminate the need for large quantities of dialyzing solutions.17 A typical home hemodialysis machine weighs 160 lbs and reaches 52 inches in height. 18 Continuously recycling the dialysis solution using hyperfiltration by reverse osmosis membranes allows a standard hemodialysis machine to become small enough to be both portable and wearable. Improving the ability of the RO membrane to reject urea could allow these devices to become even more compact.

In addition to urea, boron is another SNM that is of interest for separation. Primarily, boron is produced by the natural weathering of clay-rich sedimentary rocks. 19 While boron is an important element in humans' diet, long-term consumption of water or food with increased boron concentrations can

negatively impact the cardiovascular, coronary, nervous, and reproductive systems.²⁰⁻²² The concentration of boron in the sea is as high as 4 to 5 mg L⁻¹. ¹⁹ The guideline value for boron concentration in drinking water established by the World Health Organization is 2.4 mg L⁻¹. As a result, in order to use RO membranes to generate potable water from seawater to combat the shortage of freshwater resources, both desalination and boron separation must occur.²³

Many methods have been studied for the separation of aqueous urea and boron. Current methods used to remove aqueous solutions include decomposition, adsorption, and electro-chemical oxidation.²⁴ However, these methods are either energy-intensive, or they require complex biological processes.²⁵ Additionally, decomposition processes produce additional waste, making the treatment process more expensive and complex.²⁶ Presently, there is no simple and economic technology which can be used to effectively remove boron from aqueous mediums.20 Methods that have been studied for boron separation include thermal desalination and sorption on solids. 11 Although effective in removing dissolved boron to nearly-zero concentration, thermal desalination has lost popularity as a tool for boron separation due to its high energy intensity.^{27,28} Removal of boron from aqueous solutions via sorption on solids requires a large sorbent to boron ratio, does not allow for regeneration of the sorbent, and is limited by surface-active agents.11

Membrane technologies, such as RO, offer a simple to use, cost-effective, stable, and predictable method for the separation of small molecules. 29 Additionally, membranes are capable of simultaneously removing other solutes.²⁹ However, unaltered RO membranes are unable to effectively separate aqueous SNM's due to the aggregate free volume holes within the polyamide layer. Unaltered RO membranes are only able to produce urea rejections anywhere from 20-60% and boron rejections anywhere from 20-90%, depending on pH.13,30 Reducing this aggregate free volume space would allow the advantages of membrane technologies to be utilized for the treatment of SNM contaminated water.

The goal of this study was to improve the ability of RO membranes to separate aqueous SNMs by reducing the aggregate free-volume space on the surface of the polyamide layer. We tested the hypothesis that exploiting not fully reacted TMC molecules via carbodiimide activation and subsequent reaction with an amine would reduce the free volume space on the surface of RO membranes and improve SNM rejection. Additionally, based on previous our work,³¹ we tested the hypothesis that combining diamine or a branched polyamine coupling with thermal treatment would further improve the size-exclusion properties of the modified membranes. In this work, we modified the surface of the Dupont XLE RO membrane with various diamines and one branched polyamine, and we studied how this modification impacted membrane performance. The modified membranes were tested for pure water permeance (PWP), NaCl rejection, urea rejection, and boron rejection using a dead-end stirred

testing cell. The membrane surface chemistry, hydrophilicity, and zeta potential were also analyzed.

2. Materials and methods

2.1 Materials

Commercially produced polyamide thin-film composite (TFC) extra low energy (XLE) RO membranes were kindly provided by Dupont Water Solutions. These membranes are made up of a polyester fabric backing, a polysulfone support layer, and a thin-film polyamide selective layer. We chose the XLE membrane because it does not have a coating that could potentially alter the carbodiimide chemistry modification pathway described in Section 2.2. Deionized water was obtained from a Millipore Synergy ultraviolet water 1-(3-Dimethylaminopropyl)-3purification system. ethylcarbodiimide hydrochloride (EDC, ≥98%), β -(Nmorpholino)-ethanesulfonic acid buffer (MES, anhydrous, ≥99%), 1,6-diaminohexane (DAH, ≥98%), and crystallized urea (ACS grade, ≥99%) were used as received from VWR. N-Hydroxysuccinimide (NHS, ≥98%) and 1,8-diaminooctane (DAO, ≥98%) were used as received from TCI chemicals. 4-(2-Hydroxyethyl)piperazine-1-ethanesulfonic acid buffer (HEPES, ≥99.5%), sodium chloride (NaCl, ≥99%), boric acid (ACS grade, $\geq 99.5\%$), and *m*-phenylenediamine (MPD, 99%) were used as received from Sigma Aldrich (Millipore-Sigma). Polyethyleneimine, branched, M.W. 10000 (PEI, 99%) was used as received from Thermo Fisher Scientific Inc.

2.2 Membrane modification

Fig. 1 depicts a schematic of the membrane modification process. A small section of dry XLE membrane was cut from the flat sheet roll. This membrane piece was immersed in DI water on a VWR Standard Analog Shaker to wash the pore filler out of the membrane pores. The membrane was kept in the DI water on the shaker plate for at least 30 min. Prior to activation, the membrane was cut into a coupon with an area of 19 cm² using a precut stencil. The stencil was sized to fit the bottom of a 250 mL beaker.

An activation solution consisting of 0.078 g EDC, 0.115 g NHS, 2.922 g NaCl, and 97 g of 10 mM aqueous MES buffer (pH 5.2), weighed using a ME403E precision balance (Mettler Toledo), was mixed in a 250 mL beaker and stirred for 10 min until the solution was homogeneous. Solution pHs were measured using a HACH HO411d pH/mV meter. The rinsed membrane was immersed in the homogeneous activation solution. The beaker was covered with Parafilm and aluminum foil to protect the membrane from light, and it was left on the shaker plate for 50 min. EDC was used to activate free carboxylic acid groups on the surface of the polyamide layer formed by hydrolysis of acid chlorides at unreacted TMC sites.32 Because the resulting O-acylisourea intermediate is not water stable, NHS was used.32 After the carboxylic acid group is activated with EDC, NHS immediately replaces EDC, forming a water-stable NHS-ester intermediate.32 This intermediate is now activated for diamine coupling.

While the rinsed membrane reacted in the activation solution, the amine solution for the cross-linking step of the modification was prepared. The amine solution consists of 2 g amine (MPD – pH 7.1, DAH – pH 12.0, DAO – pH 12.0, or PEI – pH 10.8), 0.876 g NaCl, and 97 g of 10 mM aqueous HEPES buffer. The amine solution was mixed in a 250 mL beaker and stirred to homogeneity. Following the 50 min activation step, the membrane coupon was immersed in the amine solution. The cross-linking solution was covered with Parafilm and aluminum foil, and it was left on the shaker plate for 24 h. During this step, the NHS-ester intermediate reacts with the amine to form a new amide bond.

After 24 h, the amine had conjugated to active sites on the surface of the membrane. The membrane was then thoroughly rinsed with DI water to remove any unreacted amine from the surface of the membrane. Following rinsing, membranes which did not undergo heat treatment were stored in DI water, covered with Parafilm, and kept in a dark place until testing. When applicable, a heating step was performed. Half of the heat-treated membranes were treated using a standard kitchen BLACK+DECKER (Model No. – EM925AZE-P) microwave oven. For this process, the cross-linked membrane was placed in 100

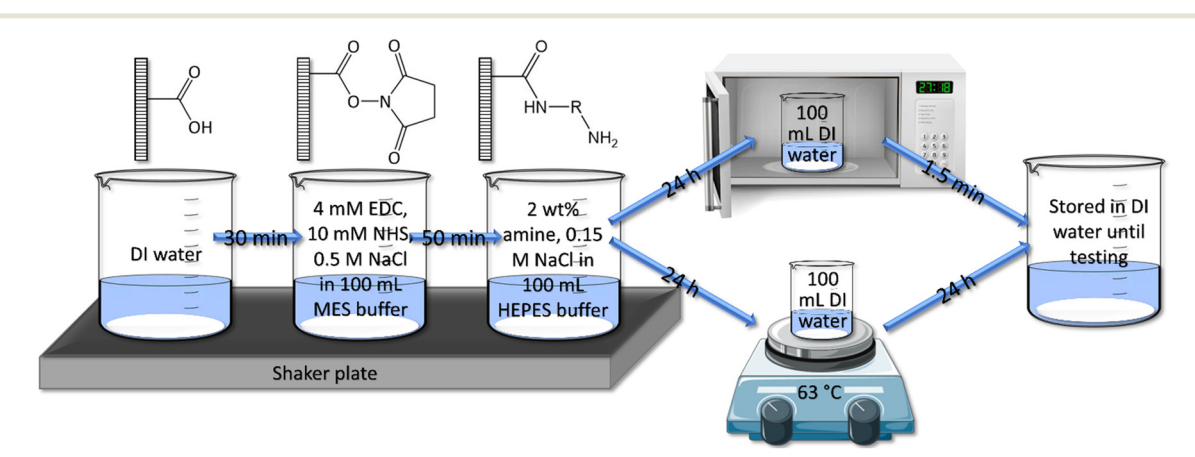


Fig. 1 Modification of polyamide layer reaction schematic. EDC/NHS is used to activate the carboxylic acid groups of the polyamide layer to allow for amine coupling which is followed by heat treatment.

Published on 11 October 2023. Downloaded by University of Alabama at Tuscaloosa on 10/27/2023 3:33:01 PM

mL DI water in a 250 mL beaker and microwaved on high, uncovered for 1.5 min. We used the microwave to reduce the processing time of the heating step from 24 h in our previous work to 1.5 min.31 During this procedure, the water in the beaker begins to visibly boil after ~45 s. Immediately following the microwave treatment, the membrane was carefully removed from the hot water using tweezers, and it was transferred to another beaker containing clean, room-temperature DI water. This beaker was covered in Parafilm and stored in a dark place until testing.

The other half of the heat-treated membranes were treated using a VWR professional hot plate stirrer (7×7 Cer Hot/Stir 120 V ADV) as a comparison to our previous work.³¹ For this process, a 250 mL beaker was filled with 100 mL DI water and placed on the hot plate which was set to a temperature of 80 °C. The DI water was heated until its temperature equilibrated at 63 °C. Then, the rinsed cross-linked membrane was immersed in the hot water. The beaker was then topped with a glass Petri dish and wrapped with aluminum foil to insulate the solution. After 24 h, the solution was removed from the hot plate, the membrane was removed from the hot water using tweezers, and the membrane was immersed in clean, room-temperature DI water and stored in a dark place until testing. The membranes will be discussed with the acronyms provided in Table 1. It should be noted that the EDC/NHS activated membranes were not tested as a control because the hydrolysis of the NHS ester can happen in a matter of minutes to hours, depending on the solution pH.33

2.3 Membrane testing

The control and modified XLE membranes were tested using a Sterlitech HP4750 dead-end filtration cell (Sterlitech, USA). The dead-end cell has a cell volume of 270 mL, and it has an effective filtration area of 14.6 cm². Prior to testing, the membranes were cut into circles with an area of ~17.4 cm² to fit the test cell. The cell was pressurized to 150 psig using either compressed nitrogen gas or air (AirGas). The

Table 1 Acronyms for the XLE membranes

Membranes	EDC/NHS	Heat treatment	Amine
Control XLE (XLE-RT)	Not used	None	None
XLE-HP	Not used	Hot plate at 63 °C	None
XLE-MW	Not used	Microwave	None
XLE-DAH	Used	None	DAH
XLE-DAH-HP	Used	Hot plate at 63 °C	DAH
XLE-DAH-MW	Used	Microwave	DAH
XLE-DAO	Used	None	DAO
XLE-DAO-HP	Used	Hot plate at 63 °C	DAO
XLE-DAO-MW	Used	Microwave	DAO
XLE-MPD	Used	None	MPD
XLE-MPD-HP	Used	Hot plate at 63 °C	MPD
XLE-MPD-MW	Used	Microwave	MPD
XLE-PEI	Used	None	PEI
XLE-PEI-HP	Used	Hot plate at 63 °C	PEI
XLE-PEI-MW	Used	Microwave	PEI

membranes were challenged with DI water, 2000 ppm aqueous NaCl (pH 6.0), 500 ppm aqueous urea (pH 6.3), and 40 ppm aqueous boric acid (pH 6.1). Each solution was allowed to permeate through the membrane for at least 30 min to achieve steady state before collection of permeate began. Approximately 10 mL of permeate was collected for each test. The time required to obtain the permeate was recorded to calculate the membrane permeance. Then, the mass of permeate obtained in that time was measured. At least three of each membrane were tested for statistical relevance. The water permeance (A) of each membrane when challenged with DI water was calculated using eqn (1).

$$A = \frac{\text{Flux}}{\text{Pressure}} = \frac{m}{a \times t \times P} \tag{1}$$

where m is the mass of the permeate, a is the testable membrane area (14.6 cm 2), t is the permeate collection time, and P is the gauge pressure (150 psi). The units of A are in L m⁻² h⁻¹ bar⁻¹ or LMH per bar.

The conductivities of the feed and permeate NaCl solutions were measured using a VWR traceable bench/ portable conductivity meter. A calibration curve was made as a function of salt concentration to ensure measurements were taken in the linear range of the conductivity meter. See Fig. S1A in the ESI† for the NaCl calibration curve. The salt rejection was calculated using eqn (2).

NaCl Rejection =
$$\left(1 - \frac{C_p}{C_f}\right) \times 100\%$$
 (2)

where C_p and C_f are the permeate and feed conductivities, respectively.

The urea feed and permeate were each diluted two times using DI water, and the absorbances of the diluted solutions were determined using a HACH DR6000 UV-vis laboratory spectrophotometer at a wavelength of 195 nm using quartz cuvettes (VWR), similar to Cheah and coworkers.34 A calibration curve was made as a function of urea concentration to ensure measurements were taken in the linear range of the UV-vis spectrophotometer. See Fig. S1B in the ESI† for the urea calibration curve. The urea rejection was calculated using eqn (3).

Urea Rejection =
$$\left(1 - \frac{Abs_p}{Abs_f}\right) \times 100\%$$
 (3)

where Abs_p and Abs_f are the permeate and feed absorbances obtained from the UV-vis spectrophotometer, respectively.

The boron feed and permeate concentrations were determined using an Agilent 5800 inductively coupled plasma optical emission spectroscopy (ICP-OES) instrument. The boron rejection was calculated using eqn (4).

Boron Rejection =
$$\left(1 - \frac{B_p}{B_f}\right) \times 100\%$$
 (4)

where B_p and B_f are the permeate and feed boron concentrations, respectively.

2.4 Membrane characterization

2.4.1 ATR-FTIR. Attenuated total reflectance Fourier-transform infrared spectroscopy (ATR-FTIR) was used to characterize the surface chemistry of the control and modified XLE membranes. The measurements were obtained using a Perkin Elmer Spectrum 2 ATR-FTIR spectrometer equipped with a diamond ATR crystal in the range of 400–4000 cm⁻¹. The data were processed using Spectrum 10 software. Each spectrum was collected for 32 scans at a resolution of 4 cm⁻¹. Each spectrum was baseline and ATR corrected with the Spectrum 10 software. All spectra were normalized to the peak at ~1490 cm⁻¹. A background of the ATR crystal was taken before testing each set of samples to ensure the crystal was clean.

2.4.2 Static contact angle goniometry. Static water contact angles were measured on the control and modified XLE membrane samples to evaluate changes in the hydrophilicity of the membrane surface. Changes in hydrophilicity can provide information about changes in surface chemistry. A contact angle goniometer (Attention Theta Lite, Biolin Scientific, Uusimaa, Finland) was used to measure all static water contact angles. A liquid drop of deionized water ($\sim\!10~\mu L)$ was carefully placed on the sample surface. For consistency, all measurements were taken 20 s after the water

droplet was placed on the surface. Measurements were done at a minimum of three locations on each sample to get a statistically relevant average contact angle.

2.4.3 Streaming potential analysis. The zeta potential of the surfaces of the control and modified XLE membranes was determined using an electrokinetic analyzer (SurPASS 3, Anton-Paar). Two membrane coupons were fixed to the sample holders of an adjustable gap cell with a gap size of $100~\mu m$ (sample size is $20~mm \times 10~mm$). In the experiment, an aqueous 0.01~M KCl solution was used as the measuring solution. For the pH adjustment, 0.05~M HCl and 0.05~M NaOH were used. The zeta potential was measured sequentially at pH 6, 9, and 3. The zeta potential was computed using the SurPASS 3 software using the Helmholtz–Smoluchowski equation. Measurements were done a minimum of three times to get a statistically relevant zeta potential value.

3. Results and discussion

3.1 Membrane performance

The control and modified XLE membranes were tested for pure water permeance, salt rejection, urea rejection, and boron rejection. The water permeance test results for membranes modified without heat treatment as well as

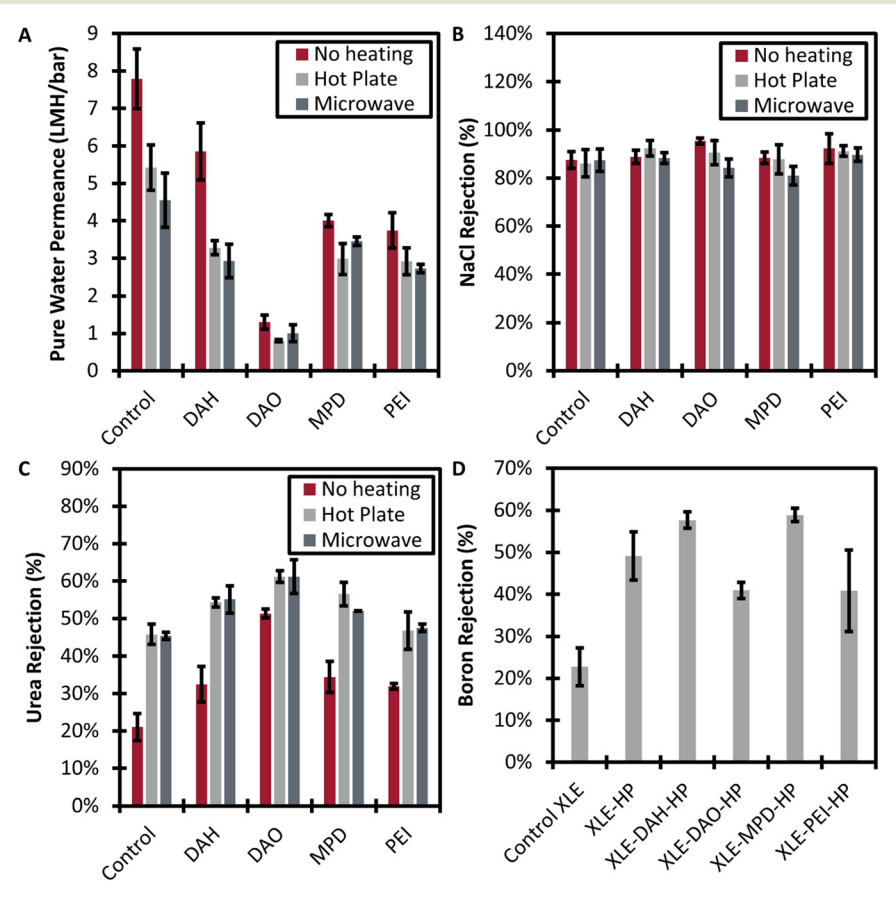


Fig. 2 Membrane performance graphs depicting (A) pure water permeance, (B) NaCl rejection, (C) urea rejection, and (D) boron rejection for the control and modified XLE membranes. The error bars represent one standard deviation among three tests.

membranes heat treated using a hot water bath or a microwave are shown in Fig. 2A. Through statistical analysis (see Table S1 in the ESI†), it was found that amine-modified XLE membranes that did not undergo heat treatment and those which underwent heat treatment via the hot plate had statistically lower pure water permeance than the XLE-RT and XLE-HP membranes. The statistical decrease in pure water permeance between the control and amine modified XLE membranes (modified without heat treatment and using the hot plate) may be explained by increased cross-linking and a likely decrease in the free volume hole size within the polyamide layer. This improved cross-linking was likely brought about via amine coupling and/or thermal rearrangement. In the case of amine-modified membranes treated using the microwave, except for the XLE-DAO-MW membranes, the water permeance was not significantly different from the XLE-MW membranes.

The differences in water permeance between the different amine modified membranes could be attributed to a couple of factors. Firstly, it may be due to a difference in the extent of attachment of the different amines to available sites on the polyamide layer. Another possible cause of these differences could be the varying hydrophilicities of the different amines used during modification. The octanol-water partition coefficient of amines can give us an estimate regarding the hydrophobicity of the amines (see Table S6 in the ESI†). The higher the octanol-water partition coefficient value, the higher the hydrophobicity of the molecule. It was found that DAO had the highest octanol-water partition coefficient by far, which helps explain why DAO modified membranes exhibited the lowest water permeance.

The ability of the control and modified XLE membranes to reject NaCl is displayed in Fig. 2B. The average NaCl rejection of the control XLE membrane was found to be 86.5%. This value was lower than the expected value of 97% provided by the manufacturer. This difference in NaCl rejection can likely be explained by the concentration polarization associated with dead-end filtration, in contrast to less sensitive cross-flow filtration.³⁵ It was found that the salt rejection exhibited by all but one of the modified membranes was not statistically different (see Table S2 in the ESI†) from the salt rejection exhibited by the unaltered, control XLE membrane. Only the XLE-DAO-RT membrane showed a statistically significant increase in NaCl rejection from the control XLE membrane. These results indicate that the modification of the membranes does not significantly impair the salt rejecting properties of the XLE membranes.

In Fig. 2C, the urea rejection is shown for both the control and modified XLE membranes. According to statistical analysis, the urea rejection of the membranes modified with amines at room temperature increased significantly (see Table S3 in the ESI†) from the control XLE membranes, suggesting that amine coupling alone improves the ability of the membrane to reject urea. Thermal treatment alone also improved the ability of the membrane to reject urea, as demonstrated by the statistical increase in urea rejection for

the XLE-HP and XLE-MW membranes compared to the control membranes.³¹

While amine coupling and thermal treatment alone were effective, the combination of both modifications provided the greatest improvement in urea rejection as demonstrated by the fact that each of the modified membranes treated with the hot plate and microwave had a higher average urea rejection than their counterparts which did not undergo heat treatment, except for the PEI-modified membranes. We believe the PEI was not attached to a large extent to XLE membranes, which was indicated in ATR-FTIR spectra (see Fig. 3). Also, it was found that the membranes modified using the hot plate had a comparable urea rejection to their counterparts modified using the microwave. Among all the membranes, the membranes modified with DAO and heat treatment exhibited the greatest average urea rejection of ~61%.

In addition to the urea rejection performance of the modified membranes, the boron rejection performance of the membranes was also evaluated. The boron rejection for the control and modified XLE membranes is shown in Fig. 2D. The hot plate treated amine-modified membranes were chosen for the boron rejection testing due to their superior performance in urea separation. According to statistical analysis, the boron rejection of the membranes modified with amines using the hot plate increased significantly (see Table S4 in the ESI†) from the control XLE membranes. Among all of the membranes, the XLE-MPD-HP modified membrane exhibited the greatest average boron rejection. Surprisingly, the DAO-modified membranes showed significantly lower boron rejection compared to the DAH-modified membranes and MPD-modified membranes.

Although boric acid and urea are both small molecules, their chemical properties and interactions with the DAOmodified membranes may be different. It is possible that the difference in the octanol-water partition coefficient of boric acid (-0.509) and urea (-1.364) may be the cause behind the difference in the urea rejection and boron rejection performance of DAO-modified membranes. The higher octanol-water partition coefficient value of boric acid molecules makes them more hydrophobic compared to urea molecules. DAO has a higher octanol-water partition coefficient compared to DAH, MPD, and PEI (see Table S6 in the ESI†), which made the modified membrane surface slightly more hydrophobic compared to other modified membranes. Huang et al. showed that the hydrophobic membrane tends to reject a lower percentage of hydrophobic solutes compared to hydrophilic solutes which may happen due to their hydrophobic adsorption followed by diffusion and/or convection through the polyamide surface.36 This could be a reason why the DAO-modified membranes exhibited a lower boron rejection compared to the urea rejection.

The modification of the XLE membranes with linear diamines showed comparable or in some cases better SNM rejection compared to the aromatic amine. It appears that the flexibility of the linear diamine better facilitates the

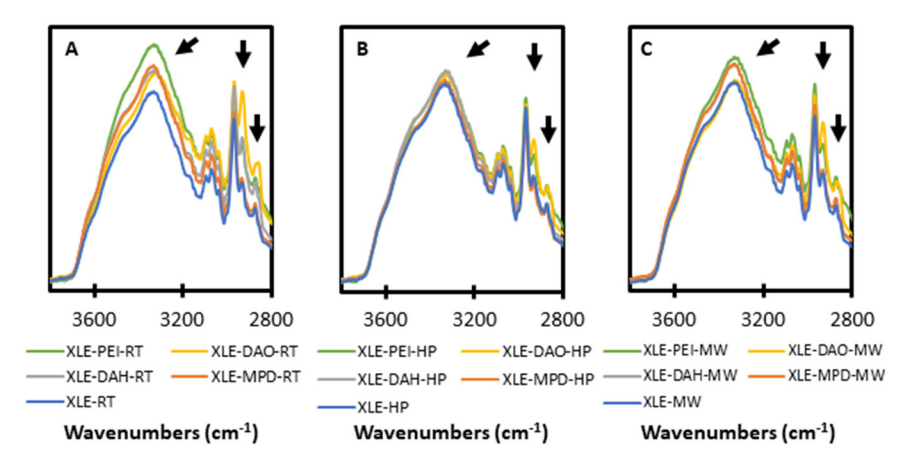


Fig. 3 ATR-FTIR spectra of (A) XLE membranes modified with/without amines and no heat treatment (B) XLE membranes modified with/without amines and then heat treated with the hot plate, and (C) XLE membranes modified with/without amines and then heat treated with the microwave.

linking mechanism between amines and unreacted carboxylic groups of the polyamide surface as compared to the aromatic diamine.³⁷ Considering the high pK_a values of the linear amines compared to the aromatic amine (see Table S6 in the ESI†), besides having stable amide linkage, there is a possibility that the unreacted end of the linear diamines formed ion pairs with the remaining free carboxylic acid groups ($pK_a \sim 4$ –5) at intermediate pHs, which may play a role in reducing the free volume.³⁷

3.2 Membrane characterization

3.2.1 ATR-FTIR. Membrane surface activation was done using carbodiimide chemistry to activate the carboxylic acid groups on the surface of the polyamide layer. In this work, commercial membranes were modified using DAH, DAO, MPD, and PEI. By combining carboxylic acid groups with amines, a new amide bond was formed. The ATR-FTIR spectra (2800–3800 cm⁻¹ range) of the control and modified XLE membranes modified at room temperature and using a hot plate or microwave are shown in Fig. 3A–C.

Characteristic peaks appeared for each membrane at $\sim 1660~{\rm cm}^{-1}$, $\sim 1610~{\rm cm}^{-1}$, and $\sim 1540~{\rm cm}^{-1}$ (see the arrows in Fig. S2 in the ESI†). These peaks correspond to the amide I, aromatic amide, and amide II bands present on the polyamide layer, respectively.³⁸ No shift or change in peak position was observed in amine-modified membranes compared to the control membrane. However, the amine-modified membranes showed very slightly more intense peaks at the amide I, aromatic amide, and amide II bond peaks.

Besides the increase in peak intensity at ~1660 cm⁻¹, ~1610 cm⁻¹, and ~1540 cm⁻¹, an increase in peak intensity at ~3330 cm⁻¹ and in the aliphatic -CH₂- stretching region of 2800-3000 cm⁻¹ also was observed (as indicated with arrows in Fig. 3). Increasing peak intensities in the region of 2800-3000 cm⁻¹ correspond to the conjugation between amines and free carboxylic acid groups. The N-H stretching at 3330 cm⁻¹ indicates the presence of amine groups on the polyamide surface. Membranes which did not undergo heat

treatment exhibited similar peak intensities at 3330 cm^{-1} and in the aliphatic $-\text{CH}_2-$ stretching region of $2800-3000 \text{ cm}^{-1}$ as membranes which were heat treated using the hot plate or the microwave. This indicates that the thermal treatment did not change the relative number of functional groups on the membrane.

Since PEI contains a greater number of N-H bonds than DAH, DAO, or MPD, PEI-modified XLE membranes exhibited the greatest N-H stretching. Additionally, it was expected that PEI-modified membranes would have the maximum intensity in the aliphatic -CH₂- stretching region of 2800–3000 cm⁻¹. However, the peaks in the aliphatic stretching region for PEI were similar to that of DAO modified membranes. This indicated that the extent of PEI attachment to the XLE membrane was not as expected, which was also reflected in the membrane performance. As compared to the control membrane, MPD-modified membranes exhibited very similar peak intensities in the aliphatic -CH₂- stretching region; however, their peak intensities were comparatively lower than those of DAH-, DAO-, or PEI-modified membranes.

3.2.2 Static angle contact angle goniometry. An analysis of static water contact angles was conducted to determine how the modification affected the hydrophobicity/hydrophilicity of XLE membranes. The water contact angle data for the modified XLE membranes which did not undergo heat treatment and modified XLE membranes which were heat treated using a hot plate or a microwave are shown in Fig. 4. A statistical difference in the water contact angles was observed between the amine-modified membranes and the control XLE membrane. It was found that DAH-, DAO-, and MPD-modified membranes had a higher water contact angle than the control XLE membranes, indicating an increased hydrophobicity of the polyamide layer. Statistical analyses are shown in Table S5 of the ESI† data. The SEM images of the membranes (see Fig. S3-S5 in the ESI†) showed the typical RO membrane ridge-and-valley structures with no visible differences in surface morphology of the modified membranes compared to the control membrane. So, we assumed that the surface roughness was similar for all

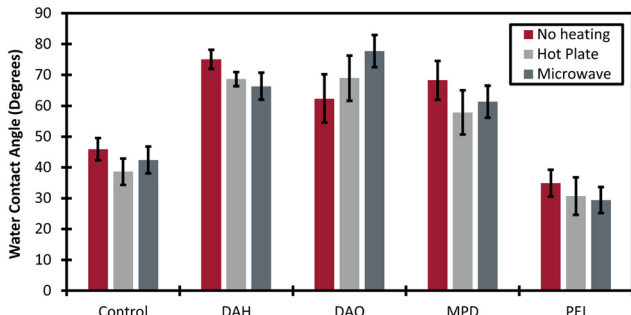


Fig. 4 Static water contact angle for the control and modified XLE membranes. The error bars represent one standard deviation among three membrane samples.

membranes. By attaching an amine, hydrophilic carboxylic acid moieties were decreased, and hydrophobic aliphatic chains or aromatic rings were increased when the membranes were modified with DAH, DAO, or MPD. There was a significant decrease in water contact angle for the PEI-modified membranes compared to control and other amine modified membranes. This reduction can be attributed to the abundance of -NH- and -NH₂ groups in PEI. The contact angles of membranes which underwent heat treatment *via* either a hot water bath or a microwave did not differ significantly from those membranes which did not undergo heat treatment.

3.2.3 Streaming potential analysis. The zeta potential of each membrane was measured sequentially at pH 6, 9, and 3 to examine the effect of amine modification on membrane surface charge. The results from the zeta potential analysis can be found in Fig. 5. Both the control and modified XLE membranes exhibited positive surface charges at pH 3. It was found that at pH values of 3, 6, and 9, the amine modified XLE membranes displayed more positive surface charges than the control XLE membrane. At pH 9, the modified XLE membranes exhibited a reduced negative surface charge. This

is likely a result of the protonated amine groups from the newly incorporated amine molecules having a greater positive charge density than the negatively charged deprotonated carboxylic acid groups.

We compared the zeta potentials of the amine-modified membranes which underwent no heat treatment, heat treatment in a hot water bath, and heat treatment in a microwave. The membranes which were modified with linear diamines or a branched polyamine showed more positive surface charges in all pH values compared to the control and MPD-modified membranes. We believe the pK_a value of the amines plays an important role in the difference between the zeta potential value of membranes modified with linear diamines or PEI and membranes modified with aromatic diamines. The pK_a values of the linear diamines and PEI were found to be higher than MPD (see Table S6 in the ESI†). This explains why there are more positive surface charges at all pH values for membranes modified with DAH, DAO, or PEI as compared to the control membranes and membranes modified with MPD.

3.3 Mechanism

Fig. 6 shows the proposed modification schematic for the XLE membranes using the carbodiimide chemistry. As mentioned previously, polyamide membranes exhibit incomplete crosslinking due to the fast, chaotic nature of the IP reaction. This can lead to sizeable free volume holes in the polyamide layer as depicted in the left-most image of Fig. 6. Werber *et al.* have demonstrated that the XLE membrane has more free carboxylic acid groups than most other RO membranes, indicating more uncross-linked areas in the membrane.³⁹ Additionally, the EDC–NHS coupling approach should modify almost exclusively the surface –COOH groups due to EDC and NHS being larger molecules than what typically permeates through the membrane.

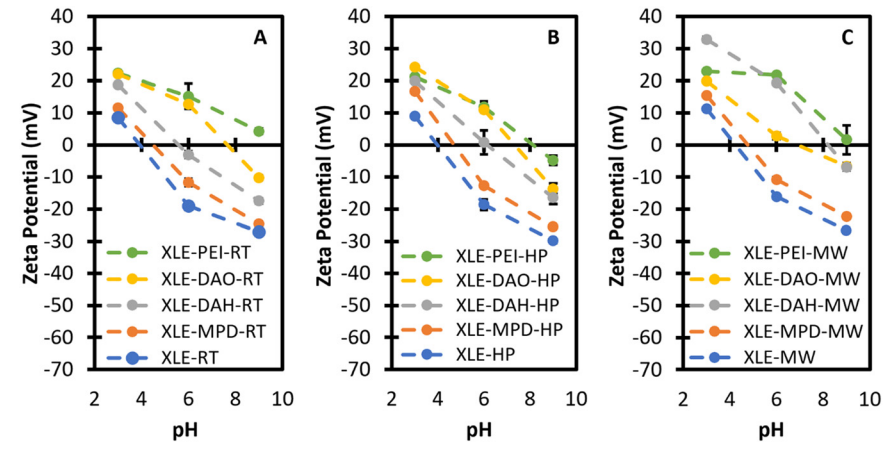


Fig. 5 Zeta potential of (A) XLE membranes modified with/without amines and without heat treatment, (B) XLE membranes modified with/without amines and then heat treated with the hot plate, and (C) XLE membranes modified with/without amines and then heat treated with the microwave, at pH 3, pH 6 and pH 9. The error bars represent one standard deviation among three tests. The dashed lines between data points are included to aid in the visual comparison of the different modifications.

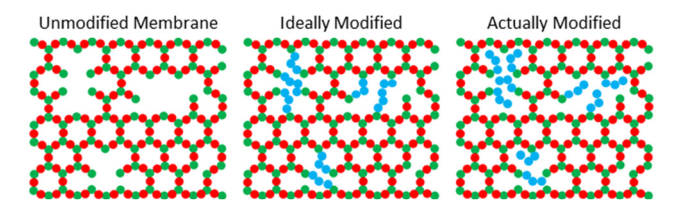


Fig. 6 Proposed modification mechanism using carbodiimide chemistry on XLE membranes. The green circles are TMC, the red circles are MPD, and the blue chains are the diamines.

In an ideal world, the amine coupling would facilitate such that one amine couples to two free carboxylic acid groups on the membrane (see center image of Fig. 6). However, to achieve this, one would need to use a tiny amount of amine. Using the data reported by Werber et al., the free carboxylic group density is 37 groups per nm² for the XLE membrane, resulting in approximately 6.42 × 10¹⁰ carboxylic acid groups present on a membrane area of 1735 mm² (the area of a 47 mm diameter circle used in the dead-end cell).³⁹ Note that this number is higher than what is likely accessible to the EDC-NHS coupling chemistry on the membrane surface, but we will move forward with it nonetheless. That means to have a 2:1 ratio between free carboxylic acid groups and diamines, 3.21×10^{10} diamine molecules are needed in the reaction solution (assuming a 100% reaction efficiency). In a 100 mL reaction solution using DAO, this means approximately 5.33 × 10^{-14} moles of DAO are needed or a wt% of 7.7 × 10^{-10} . Needless to say, these numbers are incredibly low and many orders of magnitude lower than the 2 wt% we used in this study. Therefore, the center mechanism is unlikely to occur at a significant level in our study.

Thus, the modification depicted in the right-most image of Fig. 6 is the most likely scenario that is occurring. There are more than enough amines to have one diamine coupled to each carboxylic acid group present on the membrane surface. These diamines are filling in some of the free volume space causing the demonstrated increase in small molecule rejection. We are attempting to determine the free volume hole size of these membranes using PALS, which will be shared in a future communication from our lab.

4. Conclusion

In this work, commercial RO membranes were chemically modified and heat treated to enhance the rejection of SNMs. Unexploited carboxylic acid groups on the surface of the polyamide layer were activated using carbodiimide chemistry. An amine was subsequently coupled to activated attachment sites on the surface of the membrane. Various types of diamines as well as a branched polyamine were evaluated. Amine attachment was followed by heat treatment using either a microwave or a hot water bath. Compared to control XLE membranes with a 21% urea rejection, modified XLE membranes had a 32–61% urea rejection rate, depending on the amine type and the nature of heat treatment.

For the urea rejection test, the DAO-modified membranes without heat treatment and heat treated with either a microwave or hot water bath showed significantly higher urea rejection compared to the other membranes modified without and with heat treatment. Among all the heat-treated amine modified membranes, we saw the lowest average urea rejection of 47% for the PEI-modified membranes. The urea rejection of the membranes modified with the hot plate did not show any significant difference from the urea rejection of the membranes modified with the microwave. Therefore, the microwave is a time effective way to achieve the benefits of the 24 h heat treatment in 1.5 min. In the case of the boron rejection, the modified membranes showed significantly higher boron rejection (41-59%) compared to the control XLE membranes (23%). The water permeance of the modified membranes decreased (by 25-90%) significantly from that of the control XLE membrane, as is expected with a reduced free volume space. The salt rejecting performance of the control XLE membrane was maintained in the modified membranes. The XLE-DAH-HP and XLE-MPD-HP membranes showed the best average results with pure water permeances of 3.3 and 3.0 LMH per bar, NaCl rejections of 93% and 88% (similar to or greater than the pristine XLE membrane), but with the fourth and third highest urea rejection of 53% and 57% (compared to 61% as the highest) and the highest boron rejections of 58% and 59%.

Even though we observed a reduction in the pure water permeance, even the lowest water permeance (provided by hot plate treated DAO-modified membrane) was comparable to some commercial RO membranes (0.54-0.83 LMH per bar) which are generally used for seawater desalination.40 Besides treating the effluent from irrigation and fertilizer industries, we believe, our modified membranes have the potential for producing ultrapure water (UPW) used in the manufacturing industry, where the presence of SNMs creates problems with manufacturing desired products. For example, in 1992, at Intel Corporation in the US, defective products were manufactured and an investigation revealed that the defect was caused by inadequate removal of urea from the UPW process.41 Currently, we are exploring alternative chemical modification strategies, including evaluating the effects of different surfactants during RO synthesis to increase SNM rejection and water permeance. We also are working to estimate the change in free volume hole size using PALS measurements.

Data availability

Data will be made available on request.

Author contributions

Shahriar Habib: conceptualization, data curation, formal analysis, funding acquisition, investigation, methodology, validation, visualization, writing – original draft, writing – review & editing. Madison A. Wilkins: conceptualization, data

curation, formal analysis, investigation, methodology, validation, visualization, writing - original draft, writing review & editing. Steven T. Weinman: conceptualization, formal analysis, funding acquisition, methodology, project administration, supervision, validation, visualization, writing - review & editing.

Conflicts of interest

The authors declare no conflict of interest.

Acknowledgements

S. H. was supported by an Alabama EPSCoR Graduate Research Scholars Program Fellowship. The authors would like to acknowledge the financial support of the National Science Foundation (NSF) under award number OIA-1928812 and the Department of the Interior (DOI), Bureau of Reclamation (BR) under agreement number R19AC00087. We thank NSF under award number CBET-1941700 and the Alabama Water Institute for their financial support to purchase the Anton Paar SurPASS 3. Any opinions, findings, conclusions, and/or recommendations expressed in this material are those of the authors(s) and do not necessarily reflect the views of the DOI, BR or NSF. We thank Dr. Caleb Funk for kindly providing the membranes used in this study. We thank Dr. Jason Bara for the use of his ATR-FTIR instrument. We thank Dr. Milad Rabbani Esfahani for the use of his contact angle goniometer.

References

- 1 C. E. Reid and E. J. Breton, Water and ion flow across cellulosic membranes, J. Appl. Polym. Sci., 1959, 1, 133-143.
- 2 M. M. Mekonnen and A. Y. Hoekstra, Four billion people facing severe water scarcity, Sci. Adv., 2016, 2, e1500323.
- 3 K. P. Lee, T. C. Arnot and D. Mattia, A review of reverse osmosis membrane materials for desalination-Development to date and future potential, J. Membr. Sci., 2011, 370, 1-22.
- 4 L. Shen, W.-S. Hung, J. Zuo, X. Zhang, J.-Y. Lai and Y. Wang, High-performance thin-film composite membranes developed with green ultrasound-assisted interfacial polymerization, J. Membr. Sci., 2019, 570-571, 112-119.
- 5 S. H. Kim, S.-Y. Kwak and T. Suzuki, Positron Annihilation Spectroscopic Evidence to Demonstrate Enhancement Mechanism in Morphology-Controlled Thin-Film-Composite (TFC) Membrane, Environ. Sci. Technol., 2005, 39, 1764-1770.
- 6 S. Habib and S. T. Weinman, A review on the synthesis of fully aromatic polyamide reverse osmosis membranes, Desalination, 2021, 502, 114939.
- 7 M. Dalwani, N. E. Benes, G. Bargeman, D. Stamatialis and M. Wessling, Effect of pH on the performance of polyamide/ polyacrylonitrile based thin film composite membranes, J. Membr. Sci., 2011, 372, 228-238.

- 8 K. Grzebyk, M. D. Armstrong and O. Coronell, Accessing greater thickness and new morphology features in polyamide active layers of thin-film composite membranes by reducing restrictions in amine monomer supply, J. Membr. Sci., 2022, 644, 120112.
- 9 F. Pacheco, R. Sougrat, M. Reinhard, J. O. Leckie and I. Pinnau, 3D visualization of the internal nanostructure of polyamide thin films in RO membranes, I. Membr. Sci., 2016, 501, 33-44.
- 10 K. Rahmawati, N. Ghaffour, C. Aubry and G. L. Amy, Boron removal efficiency from Red Sea water using different SWRO/BWRO membranes, J. Membr. Sci., 2012, 423-424, 522-529.
- 11 M. Tagliabue, A. P. Reverberi and R. Bagatin, Boron removal from water: needs, challenges and perspectives, J. Cleaner Prod., 2014, 77, 56-64.
- 12 F. G. Donnan, The theory of membrane equilibria, Chem. Rev., 1924, 1, 73-90.
- 13 K. L. Tu, L. D. Nghiem and A. R. Chivas, Boron removal by reverse osmosis membranes in seawater desalination applications, Sep. Purif. Technol., 2010, 75, 87-101.
- 14 H. Takeuchi, H. Tanaka, L. D. Nghiem and T. Fujioka, Emerging investigators series: a steric pore-flow model to predict the transport of small and uncharged solutes through a reverse osmosis membrane, Environ. Sci.: Water Res. Technol., 2018, 4, 493-504.
- 15 P. M. Glibert, J. Harrison, C. Heil and S. Seitzinger, Escalating Worldwide use of Urea - A Global Change Contributing to Coastal Eutrophication, Biogeochemistry, 2006, 77, 441-463.
- 16 P. Zhang, C. Peng, J. Zhang, J. Zhang, J. Chen and H. Zhao, Long-Term Harmful Algal Blooms and Nutrients Patterns Affected by Climate Change and Anthropogenic Pressures in the Zhanjiang Bay, China, Front. Mar. Sci., 2022, 9, 849819.
- 17 M. A. Kraus, M. A. Frommer, M. Nemas and R. Gutman, Urea-rejecting membranes and their application in the development of a miniature artificial kidney, J. Membr. Sci., 1976, 1, 115-127.
- 18 Hemodialysis Machines, https://homedialysis.org/homedialysis-basics/machines-and-supplies/hemodialysismachines#:~:text=Home%20hemodialysis-,Size%3A,around% 20on%20built%2Din%20wheels, (accessed 10/08/2023).
- 19 S. Dong, J. Shi, Y. Liu, Y. Qu, X. Zhao, F. Liu, P. Du and Z. Sun, Boron Exposure Assessment of Desalinated Seawater on an Island in China, Int. J. Environ. Res. Public Health, 2023, 20(3), 2451.
- 20 J. Wolska and M. Bryjak, Methods for boron removal from aqueous solutions — A review, Desalination, 2013, 310, 18-24.
- 21 A. Şimşek, D. Korkmaz, Y. S. Velioğlu and O. Y. Ataman, Determination of boron in hazelnut (Corylus avellana L.) varieties by inductively coupled plasma optical emission spectrometry and spectrophotometry, Food Chem., 2003, 83, 293-296.
- 22 L. Mel'nik, I. Butnik and V. Goncharuk, Sorption-membrane removal of boron compounds from natural and waste

- waters: Ecological and economic aspects, I. Water Chem. Technol., 2008, 30, 167-179.
- 23 M. Salehi, Global water shortage and potable water safety; Today's concern and tomorrow's crisis, Environ. Int., 2022, 158, 106936.
- 24 S. Engelhardt, J. Vogel, S. E. Duirk, F. B. Moore and H. A. Barton, Urea and ammonium rejection by an aquaporinbased hollow fiber membrane, I. Water Process Eng., 2019, 32, 100903.
- 25 E. Urbańczyk, M. Sowa and W. Simka, Urea removal from aqueous solutions—a review, J. Appl. Electrochem., 2016, 46, 1011-1029.
- 26 A. Zaher and N. Shehata, Recent advances and challenges in management of urea wastewater: A mini review, IOP Conf. Ser.: Mater. Sci. Eng., 2021, 1046, 012021.
- 27 B. Van der Bruggen and C. Vandecasteele, Distillation vs. membrane filtration: overview of process evolutions in seawater desalination, Desalination, 2002, 143, 207-218.
- 28 N. Ghaffour, T. M. Missimer and G. L. Amy, Technical review and evaluation of the economics of water desalination: Current and future challenges for better water supply sustainability, Desalination, 2013, 309, 197-207.
- S. Lee and R. M. Lueptow, Membrane Rejection of Nitrogen Compounds, Environ. Sci. Technol., 2001, 35, 3008-3018.
- 30 P. Dydo, I. Nemś and M. Turek, Boron removal and its concentration by reverse osmosis in the presence of polyol compounds, Sep. Purif. Technol., 2012, 89, 171-180.
- 31 S. Habib and S. T. Weinman, Modification of polyamide reverse osmosis membranes for the separation of urea, J. Membr. Sci., 2022, 655, 120584.
- 32 D. Bartczak and A. G. Kanaras, Preparation of Peptide-Functionalized Gold Nanoparticles Using One Pot EDC/ Sulfo-NHS Coupling, Langmuir, 2011, 27, 10119-10123.

- 33 G. Hermanson, The Reactions of Bioconjugation, Bioconjugate Techniques, 3rd edn, 2013, ch. 3, pp. 229-258, DOI: 10.1016/B978-0-12-382239-0.00003-0.
- 34 W.-K. Cheah, Y.-L. Sim and F.-Y. Yeoh, Amine-functionalized mesoporous silica for urea adsorption, Mater. Chem. Phys., 2016, 175, 151-157.
- 35 E. Nagy, in Basic Equations of Mass Transport Through a Membrane Layer, ed. E. Nagy, Elsevier, 2nd edn, 2019, pp. 497-503, DOI: 10.1016/B978-0-12-813722-2.00020-0.
- 36 S. Huang, J. A. McDonald, R. P. Kuchel, S. J. Khan, G. Leslie, C. Y. Tang, J. Mansouri and A. G. Fane, Surface modification of nanofiltration membranes to improve the removal of organic micropollutants: Linking membrane characteristics to solute transmission, Water Res., 2021, 203, 117520.
- S. Shultz, M. Bass, R. Semiat and V. Freger, Modification of polyamide membranes by hydrophobic molecular plugs for improved boron rejection, J. Membr. Sci., 2018, 546, 165-172.
- C. Y. Tang, Y.-N. Kwon and J. O. Leckie, Effect of membrane chemistry and coating layer on physiochemical properties of thin film composite polyamide RO and NF membranes: I. FTIR and XPS characterization of polyamide and coating layer chemistry, Desalination, 2009, 242, 149-167.
- 39 D. Chen, J. R. Werber, X. Zhao and M. Elimelech, A facile method to quantify the carboxyl group areal density in the active layer of polyamide thin-film composite membranes, J. Membr. Sci., 2017, 534, 100-108.
- 40 Z. Ali, Y. Al Sunbul, F. Pacheco, W. Ogieglo, Y. Wang, G. Genduso and I. Pinnau, Defect-free highly selective polyamide thin-film composite membranes for desalination and boron removal, J. Membr. Sci., 2019, 578, 85-94.
- 41 J. Rydzewski and G. Carr, Advanced organics oxidationremoving urea from high-purity water, Ultrapure Water, 2003, 20, 20-26.

Supporting Information

Emerging investigators series: Post -Synthesis Modification of Reverse Osmosis

Membranes for the Enhanced Separation of Small Neutral Molecules

- 4 Shahriar Habib[†], Madison A. Wilkins[†], and Steven T. Weinman*
- 5 Department of Chemical and Biological Engineering, The University of Alabama, Tuscaloosa,
- 6 AL 35487, USA
- 7 *Corresponding author: Tel: +1 (205)-348-8516, Fax: +1 (205)-348-7558. Email address:
- 8 stweinman@eng.ua.edu

1

2

3

10

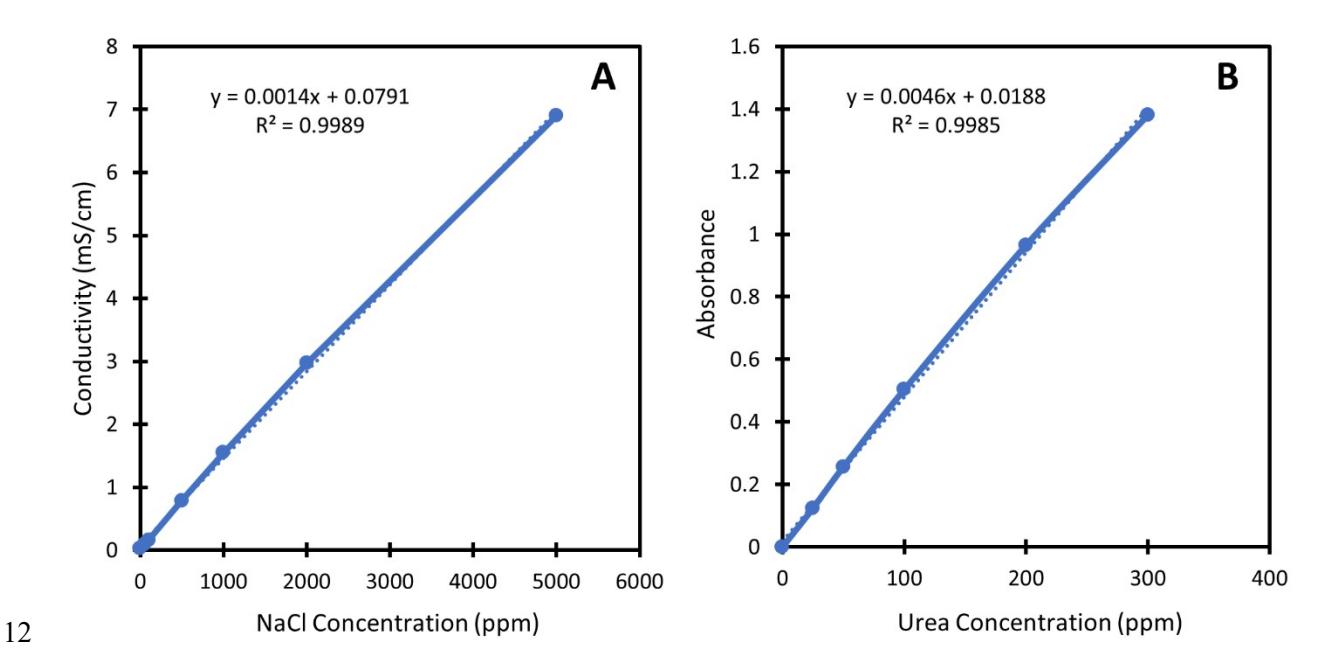
14

15

16

9 †These authors contributed equally to this work.

11 Calibration curve for NaCl solution and Urea solution



13 **Figure S1**. Calibration curve for (A) NaCl solutions and (B) urea solutions in water.

17 FTIR data (1200 cm⁻¹ - 1800 cm⁻¹ range) for XLE membranes modified using amines in post

18 modification

24

32

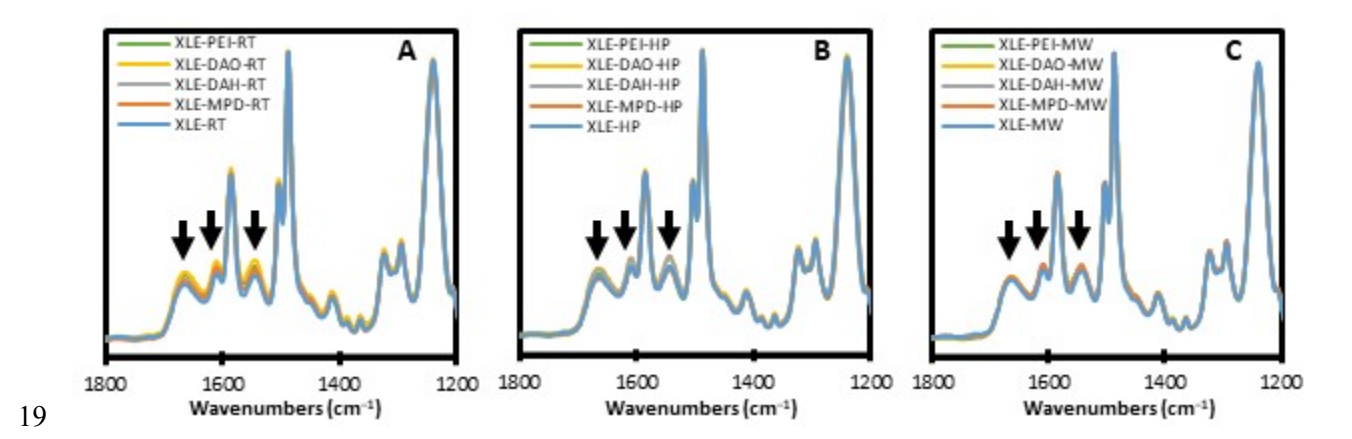


Figure S2. ATR-FTIR spectra of (A) XLE membranes modified with/without amines at room temperature, (B) XLE membranes modified with/without amines and then heat treated with the hot plate, and (C) XLE membranes modified with/without amines and then heat treated with the microwave oven.

SEM data for XLE membranes modified using amines in post modification

The control and modified XLE membrane surface morphology was studied using an Apreo field emission scanning electron microscope (FE-SEM, Thermo Fisher Scientific). The membrane samples were dried, attached with carbon tape to aluminum stabs, and sputter-coated with ~12 nm of gold (MCM-200 ion sputter coater, SEC Co., Ltd., Korea) prior to SEM imaging. The SEM images were taken at an accelerating voltage of 5 kV, a current voltage of 50 pA, and a magnification of 10,000x.

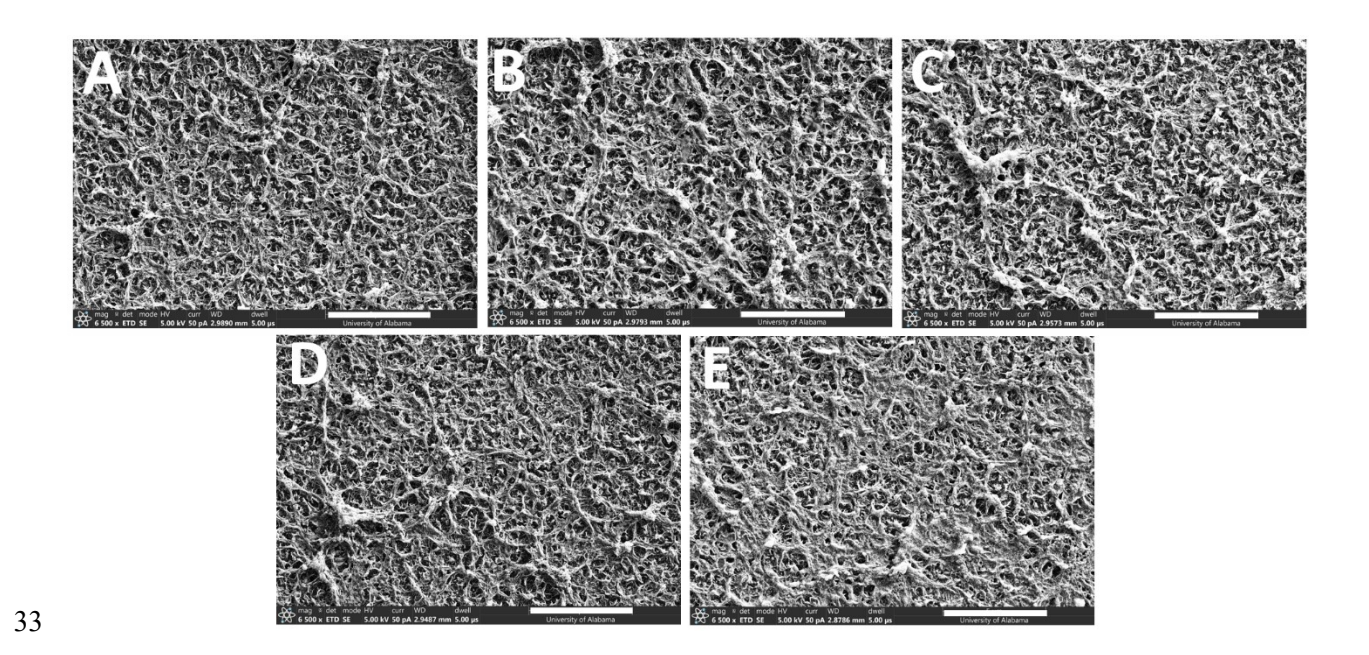
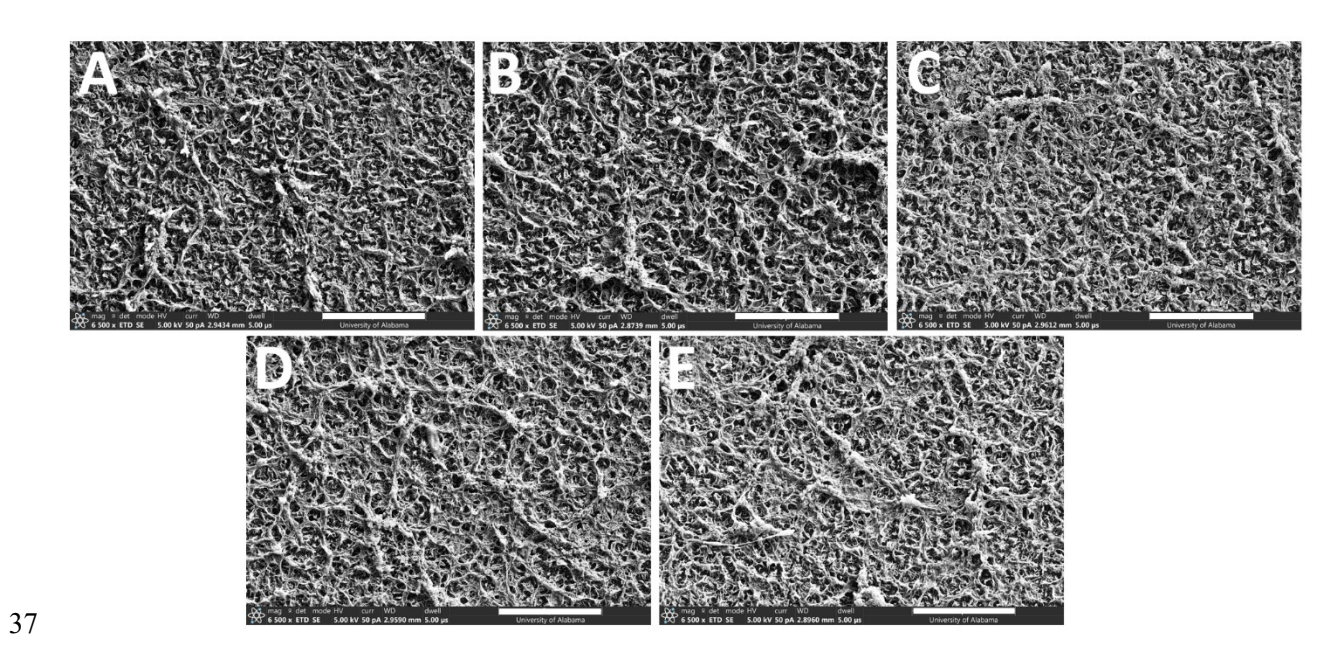


Figure S3. SEM images of (A) XLE-RT, (B) XLE-DAH-RT, (C) XLE-DAO-RT, (D) XLE-MPD-

35 RT, and (E) XLE-PEI-RT membranes. The white scale bar represents 5 μm .

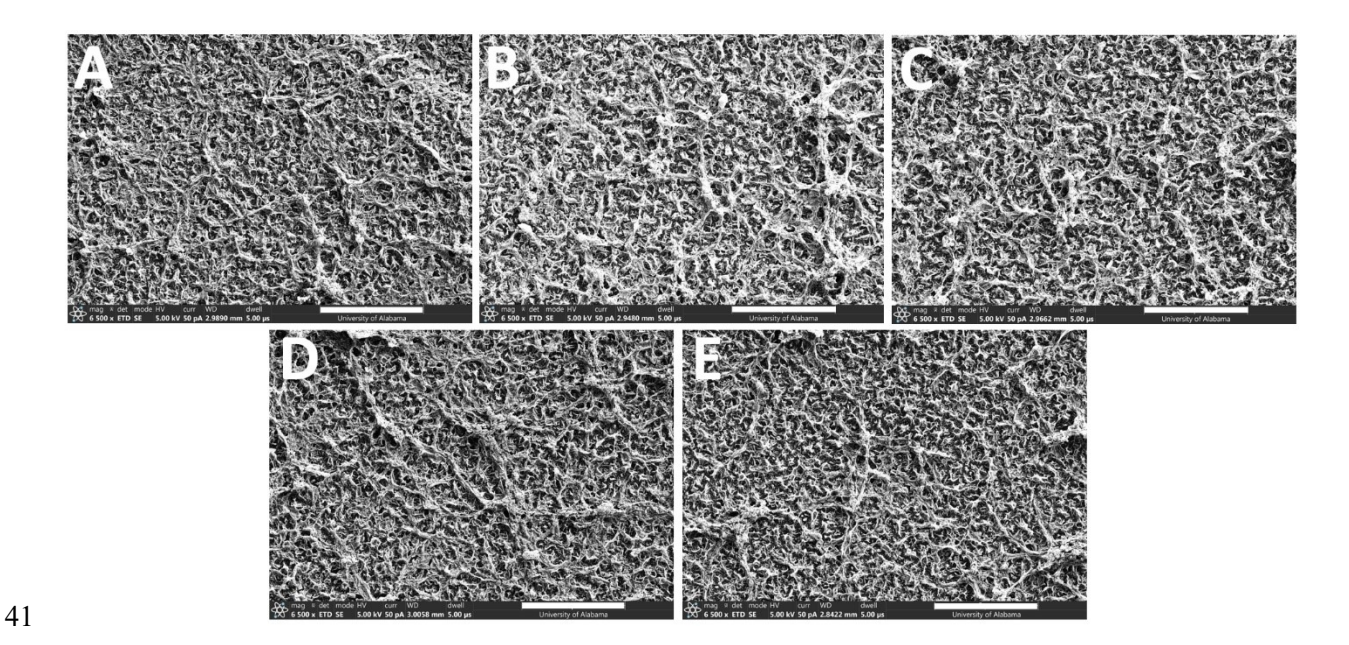


38 Figure S4. SEM images of (A) XLE-HP, (B) XLE-DAH-HP, (C) XLE-DAO-HP, (D) XLE-MPD-

39 HP, and (E) XLE-PEI-HP membranes. The white scale bar represents 5 μ m.

40

36



42 Figure S5. SEM images of (A) XLE-MW, (B) XLE-DAH-MW, (C) XLE-DAO-MW, (D) XLE-

43 MPD-MW, and (E) XLE-PEI-MW membranes. The white scale bar represents 5 μm.

45 Results of Paired t-tests

44

46 Results from Paired Two sample t-test for Means Hypothesis testing was done to determine statistical relevance of the data sets. EXCEL (Microsoft O365 Version 1908) was used for all 47 statistical analyses. All tests were done using 95% confidence ($\alpha = 0.05$); therefore, if the p-value 48 49 is greater than α then the means are considered to be equal and if the p-value is less than α then the means are considered to be unequal. Table S1 shows the results from the statistical tests on the 50 51 contact angle from Figure 3 in the main document. Table S2 and Table S3 show the results from the statistical tests on the pure water permeance and NaCl rejection data from Figures 4A, 4B, 52 53 and 4C in the main document for the 2,000 ppm NaCl feed. Table S4 shows the results from the 54 statistical tests on the urea rejection data from Figure 5 in the main document for the 500 ppm urea feed. Table S5 shows the results from the statistical tests on the boron rejection data from 55 Figure 6 in the main document for the 40 ppm boric acid feed. 56

Table S1. Results of paired t-tests on pure water permeance.

Group 1 Data	Group 2 Data	Data	Two-tailed P value	Result of Difference
XLE-RT	XLE-DAH-RT	Pure Water Permeance	0.0232	Statistically significant
XLE-RT	XLE-DAO-RT	Pure Water Permeance	0.0000	Statistically significant
XLE-RT	XLE-MPD-RT	Pure Water Permeance	0.0005	Statistically significant
XLE-RT	XLE-PEI-RT	Pure Water Permeance	0.0006	Statistically significant
XLE-HP	XLE-DAH-HP	Pure Water Permeance	0.0043	Statistically significant
XLE-HP	XLE-DAO-HP	Pure Water Permeance	0.0002	Statistically significant
XLE-HP	XLE-MPD-HP	Pure Water Permeance	0.0045	Statistically significant
XLE-HP	XLE-PEI-HP	Pure Water Permeance	0.0036	Statistically significant
XLE-MW	XLE-DAH-MW	Pure Water Permeance	0.5432	Not statistically significant
XLE-MW	XLE-DAO-MW	Pure Water Permeance	0.0051	Statistically significant
XLE-MW	XLE-MPD-MW	Pure Water Permeance	0.6928	Not statistically significant
XLE-MW	XLE-PEI-MW	Pure Water Permeance	0.3020	Not statistically significant
XLE-DAH-HP	XLE-DAH-MW	Pure Water Permeance	0.2805	Not statistically significant
XLE-DAH-RT	XLE-DAH-MW	Pure Water Permeance	0.0046	Statistically significant
XLE-DAH-RT	XLE-DAH-HP	Pure Water Permeance	0.0048	Statistically significant
XLE-DAO-HP	XLE-DAO-MW	Pure Water Permeance	0.1943	Not statistically significant
XLE-DAO-RT	XLE-DAO-MW	Pure Water Permeance	0.1499	Statistically significant

XLE-DAO-RT	XLE-DAO-HP	Pure Water Permeance	0.0105	Not statistically significant
XLE-MPD-HP	XLE-MPD-MW	Pure Water Permeance	0.1274	Not statistically significant
XLE-MPD-RT	XLE-MPD-MW	Pure Water Permeance	0.0086	Statistically significant
XLE-MPD-RT	XLE-MPD-HP	Pure Water Permeance	0.0165	Not statistically significant
XLE-PEI-HP	XLE-PEI-MW	Pure Water Permeance	0.4252	Not statistically significant
XLE-PEI-RT	XLE-PEI-MW	Pure Water Permeance	0.0219	Statistically significant
XLE-PEI-RT	XLE-PEI-HP	Pure Water Permeance	0.0743	Not statistically significant
XLE-RT	XLE-MW	Pure Water Permeance	0.0002	Statistically significant
XLE-RT	XLE-HP	Pure Water Permeance	0.0081	Statistically significant
XLE-HP	XLE-MW	Pure Water Permeance	0.0109	Statistically significant

59 Table S2. Results of paired t-tests on NaCl rejection.

Group 1 Data	Group 2 Data	Data	Two-tailed P value	Result of Difference
XLE-RT	XLE-DAH-RT	NaCl Rejection	0.6067	Not statistically significant
XLE-RT	XLE-DAO-RT	NaCl Rejection	0.0145	Statistically significant
XLE-RT	XLE-MPD-RT	NaCl Rejection	0.7274	Not statistically significant
XLE-RT	XLE-PEI-RT	NaCl Rejection	0.2442	Not statistically significant
XLE-HP	XLE-DAH-HP	NaCl Rejection	0.1662	Not statistically significant
XLE-HP	XLE-DAO-HP	NaCl Rejection	0.3582	Not statistically significant

XLE-HP	XLE-MPD-HP	NaCl Rejection	0.7392	Not statistically significant
XLE-HP	XLE-PEI-HP	NaCl Rejection	0.2135	Not statistically significant
XLE-MW	XLE-DAH-MW	NaCl Rejection	0.5852	Not statistically significant
XLE-MW	XLE-DAO-MW	NaCl Rejection	0.4429	Not statistically significant
XLE-MW	XLE-MPD-MW	NaCl Rejection	0.1246	Not statistically significant
XLE-MW	XLE-PEI-MW	NaCl Rejection	0.3394	Not statistically significant
XLE-DAH-HP	XLE-DAH-MW	NaCl Rejection	0.1392	Not statistically significant
XLE-DAH-RT	XLE-DAH-MW	NaCl Rejection	0.8024	Not statistically significant
XLE-DAH-RT	XLE-DAH-HP	NaCl Rejection	0.2104	Not statistically significant
XLE-DAO-HP	XLE-DAO-MW	NaCl Rejection	0.1498	Not statistically significant
XLE-DAO-RT	XLE-DAO-MW	NaCl Rejection	0.0079	Statistically significant
XLE-DAO-RT	XLE-DAO-HP	NaCl Rejection	0.1816	Not statistically significant
XLE-MPD-HP	XLE-MPD-MW	NaCl Rejection	0.1833	Not statistically significant
XLE-MPD-RT	XLE-MPD-MW	NaCl Rejection	0.0495	Statistically significant
XLE-MPD-RT	XLE-MPD-HP	NaCl Rejection	0.8884	Not statistically significant
XLE-PEI-HP	XLE-PEI-MW	NaCl Rejection	0.4756	Not statistically significant
XLE-PEI-RT	XLE-PEI-MW	NaCl Rejection	0.5417	Not statistically significant
XLE-PEI-RT	XLE-PEI-HP	NaCl Rejection	0.8227	Not statistically significant

XLE-RT	XLE-MW	NaCl Rejection	0.7907	Not statistically significant
XLE-RT	XLE-HP	NaCl Rejection	0.6952	Not statistically significant
XLE-HP	XLE-MW	NaCl Rejection	0.8626	Not statistically significant

Table S3. Results of paired t-tests on urea rejection.

Group 1 Data	Group 2 Data	Data	Two-tailed P value	Result of Difference
XLE-RT	XLE-DAH-RT	Urea Rejection	0.0143	Statistically significant
XLE-RT	XLE-DAO-RT	Urea Rejection	0.0000	Statistically significant
XLE-RT	XLE-MPD-RT	Urea Rejection	0.0060	Statistically significant
XLE-RT	XLE-PEI-RT	Urea Rejection	0.0040	Statistically significant
XLE-HP	XLE-DAH-HP	Urea Rejection	0.0075	Statistically significant
XLE-HP	XLE-DAO-HP	Urea Rejection	0.0010	Statistically significant
XLE-HP	XLE-MPD-HP	Urea Rejection	0.0106	Statistically significant
XLE-HP	XLE-PEI-HP	Urea Rejection	0.7750	Not statistically significant
XLE-MW	XLE-DAH-MW	Urea Rejection	0.0034	Statistically significant
XLE-MW	XLE-DAO-MW	Urea Rejection	0.0009	Statistically significant
XLE-MW	XLE-MPD-MW	Urea Rejection	0.0001	Statistically significant
XLE-MW	XLE-PEI-MW	Urea Rejection	0.0374	Statistically significant
XLE-DAH-HP	XLE-DAH-MW	Urea Rejection	0.7339	Not statistically significant

XLE-DAH-RT	XLE-DAH-MW	Urea Rejection	0.0028	Statistically significant
XLE-DAH-RT	XLE-DAH-HP	Urea Rejection	0.0015	Statistically significant
XLE-DAO-HP	XLE-DAO-MW	Urea Rejection	0.9818	Not statistically significant
XLE-DAO-RT	XLE-DAO-MW	Urea Rejection	0.0216	Statistically significant
XLE-DAO-RT	XLE-DAO-HP	Urea Rejection	0.0009	Statistically significant
XLE-MPD-HP	XLE-MPD-MW	Urea Rejection	0.0675	Not statistically significant
XLE-MPD-RT	XLE-MPD-MW	Urea Rejection	0.0019	Statistically significant
XLE-MPD-RT	XLE-MPD-HP	Urea Rejection	0.0018	Statistically significant
XLE-PEI-HP	XLE-PEI-MW	Urea Rejection	0.8112	Not statistically significant
XLE-PEI-RT	XLE-PEI-MW	Urea Rejection	0.0000	Statistically significant
XLE-PEI-RT	XLE-PEI-HP	Urea Rejection	0.0070	Statistically significant
XLE-RT	XLE-MW	Urea Rejection	0.0000	Statistically significant
XLE-RT	XLE-HP	Urea Rejection	0.0002	Statistically significant
XLE-HP	XLE-MW	Urea Rejection	0.8161	Not statistically significant

Table S4. Results of paired t-tests on boron rejection.

Group 1 Data	Group 2 Data	Data	Two-tailed P value	Result of Difference
XLE-RT	XLE-DAH-HP	Boron Rejection	0.0003	Statistically significant
XLE-RT	XLE-DAO-HP	Boron Rejection	0.0031	Statistically significant

XLE-RT	XLE-MPD-HP	Boron Rejection	0.0002	Statistically significant
XLE-RT	XLE-PEI-HP	Boron Rejection	0.0428	Statistically significant
XLE-RT	XLE-HP	Boron Rejection	0.0034	Statistically significant

Table S5. Results of paired t-tests on water contact angle measurement.

Group 1 Data	Group 2 Data	Data	Two-tailed P value	Result of Difference
XLE-RT	XLE-DAH-RT	Contact Angle	0.0000	Statistically significant
XLE-RT	XLE-DAO-RT	Contact Angle	0.0009	Statistically significant
XLE-RT	XLE-MPD-RT	Contact Angle	0.0000	Statistically significant
XLE-RT	XLE-PEI-RT	Contact Angle	0.0008	Statistically significant
XLE-HP	XLE-DAH-HP	Contact Angle	0.0000	Statistically significant
XLE-HP	XLE-DAO-HP	Contact Angle	0.0000	Statistically significant
XLE-HP	XLE-MPD-HP	Contact Angle	0.0002	Statistically significant
XLE-HP	XLE-PEI-HP	Contact Angle	0.0259	Statistically significant
XLE-MW	XLE-DAH-MW	Contact Angle	0.0000	Statistically significant
XLE-MW	XLE-DAO-MW	Contact Angle	0.0000	Statistically significant
XLE-MW	XLE-MPD-MW	Contact Angle	0.0000	Statistically significant
XLE-MW	XLE-PEI-MW	Contact Angle	0.0003	Statistically significant
XLE-DAH-HP	XLE-DAH-MW	Contact Angle	0.3190	Not statistically significant

XLE-DAH-RT	XLE-DAH-MW	Contact Angle	0.0014	Statistically significant
XLE-DAH-RT	XLE-DAH-HP	Contact Angle	0.0009	Statistically significant
XLE-DAO-HP	XLE-DAO-MW	Contact Angle	0.0382	Statistically significant
XLE-DAO-RT	XLE-DAO-MW	Contact Angle	0.0025	Statistically significant
XLE-DAO-RT	XLE-DAO-HP	Contact Angle	0.1616	Not statistically significant
XLE-MPD-HP	XLE-MPD-MW	Contact Angle	0.3610	Not statistically significant
XLE-MPD-RT	XLE-MPD-MW	Contact Angle	0.0654	Not statistically significant
XLE-MPD-RT	XLE-MPD-HP	Contact Angle	0.0240	Statistically significant
XLE-PEI-HP	XLE-PEI-MW	Contact Angle	0.8634	Not statistically significant
XLE-PEI-RT	XLE-PEI-MW	Contact Angle	0.0726	Not statistically significant
XLE-PEI-RT	XLE-PEI-HP	Contact Angle	0.1938	Not statistically significant
XLE-RT	XLE-MW	Contact Angle	0.1653	Not statistically significant
XLE-RT	XLE-HP	Contact Angle	0.0102	Statistically significant
XLE-HP	XLE-MW	Contact Angle	0.1607	Not statistically significant

- 71 Minimal projection area, pKas, and Octanol water partition coefficient data of amines used
- 72 in modified XLE membranes

- 73 Table S6. Minimal projection area, pKas, and Octanol water partition coefficient data of MPD,
- 74 DAH, DAO and PEI from http://www.chemicalize.org website.)

Compound	pK _{a1}	pK _{a2}	Octanol water Coefficient
MPD	2.73	5.48	0.315
DAH	9.90	10.51	0.044
DAO	9.90	10.51	0.933
PEI	10.16		-0.279
Urea			-1.364
Boric Acid	8.70	12.11	-0.509